Surface Heterogeneity Effect on Azodyes Adsorption on to Multiwalled Carbon Nanotubes

Cassiano Rodrigues de Oliveira[*]

Federal University of Viçosa, Rio Paranaíba Campus, Brazil

Abstract: The adsorption thermodynamics of the azo dyes acid yellow 42 (AY), acid black 210 (AB) and acid green 68:1 (AG) onto pristine multi-walled carbon nanotubes (MWCNTs) was evaluated by determining the following thermodynamic adsorption parameters: adsorption standard free energy ($\Delta_{ads}G°$), adsorption standard enthalpy ($\Delta_{ads}H°$) and adsorption standard entropy ($\Delta_{ads}S°$). The adsorption of all azo dyes onto MWCNTs was a thermodynamically spontaneous process and the decrease in $\Delta_{ads}G°$ values follows the order AG < AB < AY. The increase of oxidized sites on MWCNT surface enabled a decrease of adsorption capacity of AY, compared with raw MWCNT. The adsorption of all azodyes is directly proportional with the ionic strength of solution. Isothermal Titration Calorimetry (ITC) data show that the adsorption process is enthalpically driven for all azodyes with contribution of entropy change in the spontaneity of AY adsorption onto MWCNT. The surface of the MWCNT has sites with different energetic potentials that allow electrostatic interactions with azo dye compounds, not only π−π dispersion interactions. The ITC technique provides a more reliable interpretation of the surface chemistry of MWCNT and of the interactions in an adsorption process in comparison with the van't Hoff approximation.

Keywords: Isothermal titration calorimetry, Surface modification, Wastewater treatment.

1. INTRODUCTION

Wastewater from dyeing industries, such as textiles, dyestuff, paper and leather, is a hazardous discharge because of its toxicity and environmental pollution. Dyes added to natural waters are also aesthetically objectionable for drinking and other purposes [1]. Their synthetic origins and complex aromatic molecular structure implies in low biodegradability.

Several methods are employed for dyes removal from industrial effluents, and adsorption is regarded as an efficient process because of its low initial cost, ease of operation and design flexibility and simplicity [2].

Among adsorbents applied for dyes removal [3-10], carbon nanotubes (CNTs) are becoming attractive because of the following characteristics: capacity to adsorb colored compounds from aqueous solutions [11-13] and large surface area and high porosity [14]. However, to our best knowledge there are only four papers published, reporting the adsorption thermodynamics of azo dyes on CNTs [1, 13, 15-16], none of which measuring directly the adsorption standard enthalpy by means of isothermal titration calorimetry (ITC). Machado *et al.* [1] found that the adsorption of the azo dye Reactive Red M-2BE onto multi-walled carbon nanotubes presented a maximum adsorption capacity of 312.3 mg g⁻¹ at 298 K. Although the process was endothermic ($\Delta_{ads}H° = 33.13$ kJ mol⁻¹), the positive variation in the standard entropy of adsorption ($\Delta_{ads}S° = 208.0$ J K⁻¹ mol⁻¹) guarantees the

spontaneity of the adsorption phenomenon. The authors also suggested a mechanism of adsorption with three steps: the functional groups of the MWCNTs are protonated; agglomerates of dyes are dispersed in the aqueous solution; and the negatively charged dyes are electrostatically attracted to the positively charged surface of the MWCNTs. Several works found in literature describe the thermodynamics of dye adsorption onto MWCNT, with all of them applying Van't Hoff approximation to determine $\Delta_{ads}H°$. Kuo *et al.* [13] found lower values of maximum adsorption capacity of Direct Yellow 86 (54.9 mg g⁻¹) and Direct Red 224 (52.1 mg g⁻¹) at 35 °C onto CNT. The process was endothermic ($\Delta_{ads}H° = 13.69$ kJ mol⁻¹ for DY 86; $\Delta_{ads}H° = 24.29$ kJ mol⁻¹ for DR 224), and $\Delta_{ads}S°$ was positive (139.51 and 177.83 J K⁻¹ mol⁻¹ for AY 86 and AR 224, respectively). The authors suggest that the adsorption of both dyes onto CNT was driven by a physisorption process. The same conclusion was taken by Wu [15], who studied the adsorption of Procion Red MX-5B onto CNT and found that the maximum amount dye adsorbed (Γ_{max}) ranges from 29.94 to 44.64 mg g⁻¹ between pH 6.5-10 and temperatures between 281 and 321 K. The thermodynamic properties revealed a spontaneous ($\Delta_{ads}G° = -29.79$ kJ mol⁻¹ at 281 K, pH = 6.5), endothermic process (31.55 kJ mol⁻¹ at pH 6.5), with $\Delta_{ads}S° = 216.99$ J mol⁻¹ K⁻¹. Therefore, information about the influence of MWCNT surface on the adsorption mechanism is required.

This study aims to investigate the adsorption of three azo dyes (AD) on multiwalled carbon nanotubes (MWCNT) from aqueous solutions and also describes, for the first time, the nature of CNTs surface and the interactions between CNTs and adsorbates by means of isothermal titration calorimetry.

*Address correspondence to this author at the Federal University of Viçosa, Rio Paranaíba Campus, Brazil;
E-mail: cassiano.oliveira@ufv.br

2. MATERIAL AND METHODS

2.1. Adsorbates

The adsorbates, AY [chemical formula: $C_{32}H_{24}N_8Na_2O_8S_2$, MW: 758.69 g mol^{-1}, λ_{max} = 411 nm], AB [chemical formula: $C_{34}H_{25}K_2N_{11}O_{11}S_3$, MW: 938.02 g mol^{-1}, λ_{max} = 462 nm] and AG [chemical formula: $C_{34}H_{25}N_9O_{13}S_3$, MW: 863.8098 g mol^{-1}, λ_{max} = 603 nm] were donated by BASF Corp., Brazil. The structures of AY, AB and AG dyes are illustrated in Figure **1**. An exact weighted quantity of each dye was dissolved in distilled water to prepare stock solutions (1 mg mL^{-1}). All solutions employed in the experiments were obtained by successive dilutions with distilled water.

2.2. Characterization of CNT

Multi-walled carbon nanotubes C_{TUBE} 100 were purchased from CNT CO., LTD., Korea. The following technical specification of the MWCNT was supplied by the manufacturer: average diameter: 10-40 nm; length: 1-25 μm; purity: 93 wt% min.; contaminants: 7 wt% max.; bulk density: 0.03-0.06 g cm^{-3}; specific surface area: 150-250 m^2 g^{-1}.

N$_2$ adsorption: The specific surface area and porosity were determined at 77 K with a Nova 1000 volumetric adsorption analyzer, acquired from Quantachrome Corp., USA. Brunauer-Emmett-Teller (BET) and Barret, Joyner and Halenda (BJH) methods were used to determine BET surface area and pore size distribution, respectively.
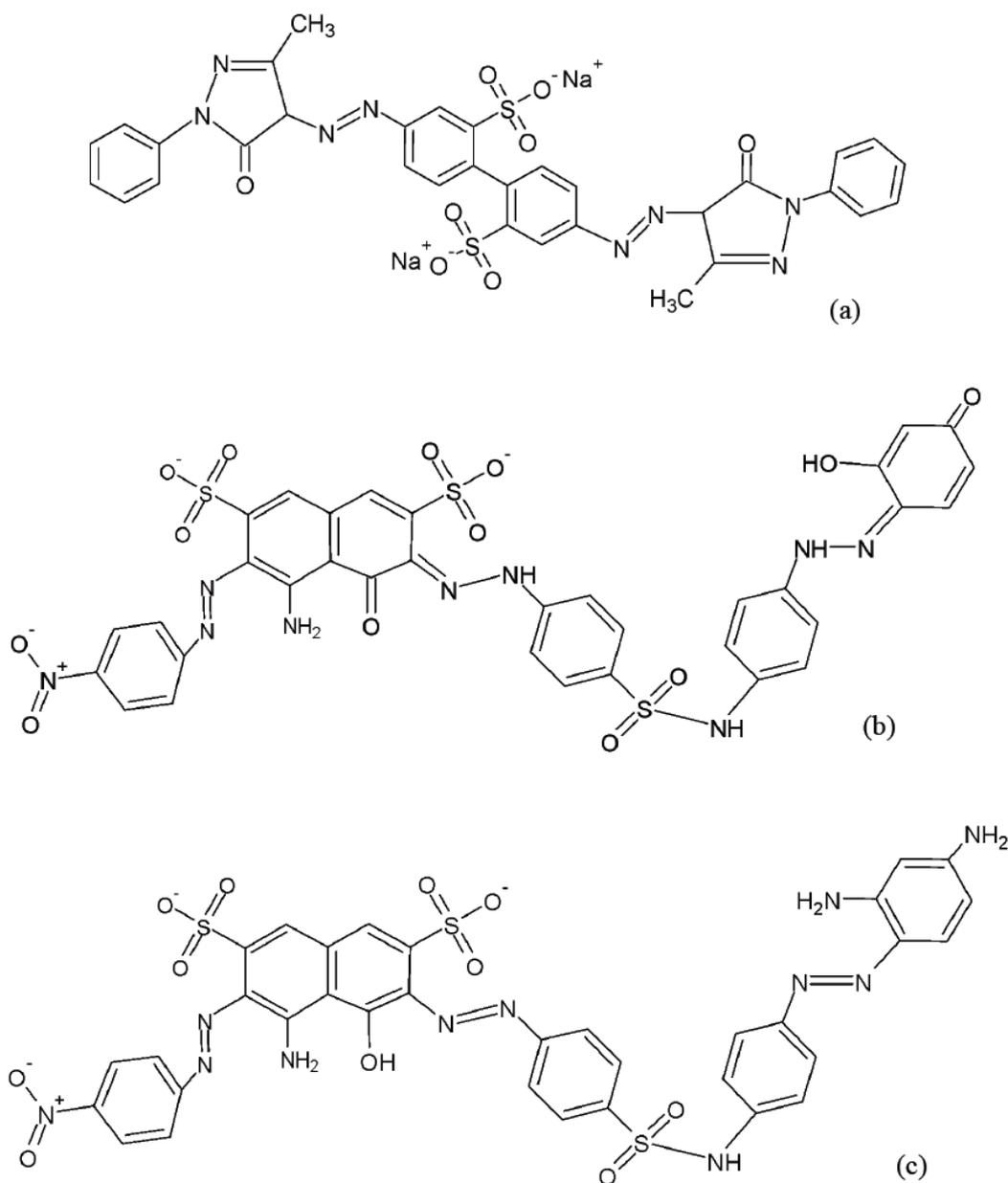

Figure 1: Molecular structures of (**a**) AY, (**b**) AG and (**c**) AB.

Thermogravimetric Analysis (TG): Thermogravimetric measurements were performed in a TA Instruments SDT 2960 simultaneous TG/DTA at 5°C min^{-1} in dry air flow of 100 mL min^{-1} between 25 and 1000 °C in alumina crucibles. The degradation temperature was determined by T_{onset}. Scanning electron microscopy (SEM) and transmission electron microscopy (TEM) were performed with a JEOL JSM-8404 scanning microscope and a JEOL JEM-2010 transmission microscope, respectively.

Transmission Electron Microscopy: Transmission electron microscopy (TEM) was carried out with a Tecnai G-20 (FEI) microscope employing a LaB$_6$ filament with an acceleration voltage of 200 kV. The samples for TEM studies were dispersed in ethanol and dripped onto a carbon-coated copper grid.

UV/Vis Spectroscopy: After the proper equilibrium time (24 h), aliquots of each flask were collected and diluted by different factors. The samples were then measured in a Thermo Scientific Evolution 300 UV/Vis spectrophotometer.

Isothermal Titration Calorimetry (ITC): Measurements of the enthalpy changes in the adsorption process of azo dyes onto MWCNT were performed in triplicate using a CSC-4200 microcalorimeter (Calorimeter Science Corp.) controlled by the ItcRun software with a 1.75 mL reaction cell (sample and reference). The entire calorimetry procedure was calibrated chemically and electrically to the heat of protonation for tris(hydroxymethyl) aminomethane and the Joule effect, respectively [20]. The titrations were carried out via step-by-step injections (10 µL) of concentrated azo dyes titrating solutions using an instrument-controlled gas-tight Hamilton syringe (250 µL) at 60-min intervals between each injection. Aliquots of concentrated azo dyes solutions, dissolved in water, were added to a sample cell containing a suspension of 1.35 mg of MWCNT in aqueous solution. The solution was titrated in the sample cell stirred at 300 rpm by a helix stirrer, and measurements were carried out at a constant temperature of 25.000 ± 0.001 °C. Distilled water was used for preparing all solutions and carbon nanotube suspensions. The concentrations of the initial dyes solutions were chosen so that after each injection, the resulting concentrations in the sample cell would become identical to the concentrations used to obtain the adsorption isotherms.

2.3. Surface Modification of CNT

MWCNT surface was modified to study the effect of oxidation on the adsorption of dye. Surface modification procedures were employed as described elsewhere [17, 18].

MWCNT acidification. 100 mL of concentrated HNO$_3$ were added to 1 g of MWCNT at constant magnetic stirring for 24 h at room temperature. This procedure yielded acidified carbon nanotubes labeled as MWCNT-acid.

MWCNT oxidation. 100 mL of H$_2$O$_2$ at 18 % (v/v) were added to 1 g of MWCNT at constant magnetic stirring for 4 h at 80 °C. Carbon nanotubes obtained by this method were labeled as MWCNT-oxid.

Modified MWCNT were filtered, washed thoroughly with distilled water and dried at (378 ± 5) K for 12 h, prior to use.

2.4. Adsorption Experiments

Adsorption experiments were carried out in duplicate with a set of 40-mL glass centrifuge tubes sealed with headspace screw caps, where solutions of dye (20 mL) with different initial concentrations (C_0) (0.01 – 0.50 mg mL^{-1}) were mixed with 15 mg of MWCNT. The tubes were shaken manually for 10 minutes and placed in a thermostatically controlled bath, at different temperatures (278.15, 288.15, 298.15, 308.15 and 318.15 K), for 24 hours to reach thermodynamic equilibrium. All experiments were performed at a constant solution pH, derived from distilled water pH (5.5). The effect of ionic strength was investigated at three levels of NaCl concentration (0.00, 0.01 and 0.10 mol L^{-1}). Blank experiments were carried out using the same experimental procedure without MWCNT to check potential adsorption of dye onto glass tubes. Separation of MWCNT and supernatants was made by centrifugation. The collected aliquots were diluted to ensure that absorbance readings obeyed Beer's Law by UV/Vis spectrophotometry. The amount of adsorbed dye on MWCNT at equilibrium, Γ (mg g^{-1}), was calculated as follows:

$$\Gamma = \left(\frac{C_0 - C_e}{m}\right) V \qquad (1)$$

where Γ is the amount of dye adsorbed onto the MWCNTs (mg g^{-1}) after thermodynamic equilibrium; C_0 and C_e are the initial and the equilibrium concentrations (mg mL^{-1}), respectively; V is the solution volume (mL); and m is the mass of MWCNT used (g).
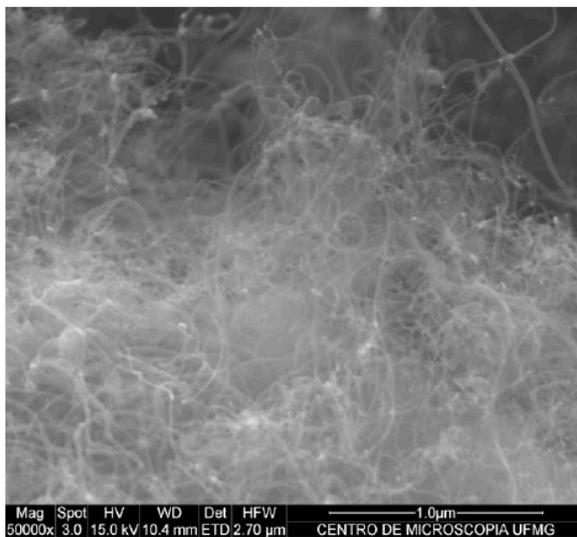
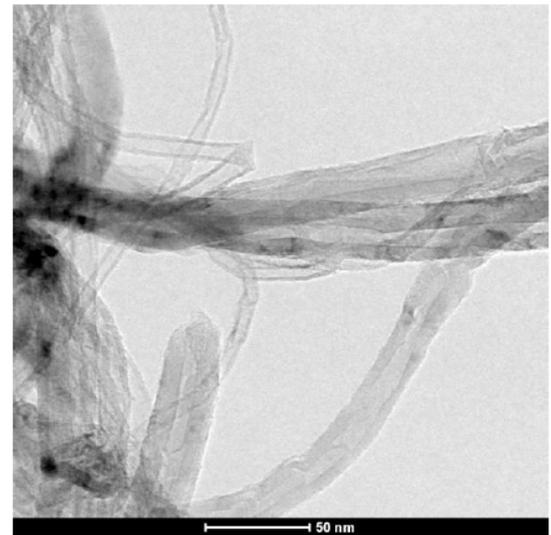## 3. RESULTS AND DISCUSSION

3.1. CNT Characteristics

The BET surface area, average mesopore and micropore volumes are 188 m^2 g^{-1}, 0.597 cm^3 g^{-1}, and 0.068 cm^3 g^{-1}, respectively. Thermogravimetric analysis, SEM and TEM micrographs are presented in Figure **2**, which shows that MWCNT has purity higher than 90 % and average diameter of 10-40 nm. These
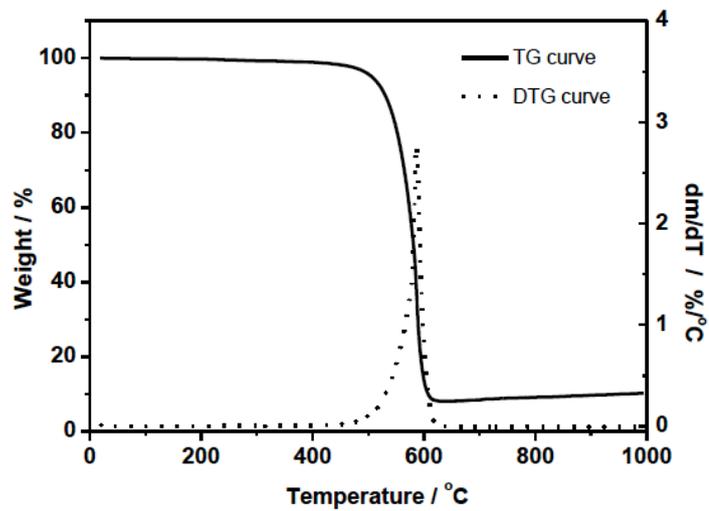
(**a**)

(**b**)

(**c**)

Figure 2: (**a**) TG e DTG curves, (**b**) SEM and (**c**) TEM micrographs.

data are consistent with the information provided by the supplier of the material, as previously presented.

3.2. Equilibrium Study

The adsorption isotherm presents the distribution of adsorbate molecules between the liquid and the solid phases at equilibrium [9]. A period of 24 h was considered to reach thermodynamic equilibrium. In fact, several reports demonstrated that adsorption of dyes onto CNTs takes place until equilibrium in the range of 100-360 min [11-15]. Figure **3** shows the amounts adsorbed (Γ) of AY, AB and AG plotted against the equilibrium concentrations (C_e) at 298 K.

All isotherms present the same nonlinear profile: an increase in the adsorbed amount with increasing equilibrium concentrations followed by a tendency to form a plateau at higher concentrations, which describes the maximum adsorption capacity. The order of adsorption follows: AG < AB < AY.
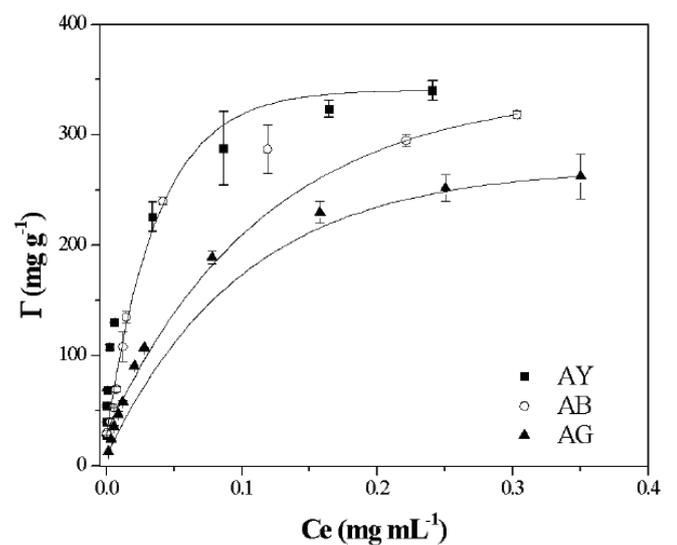

Figure 3: Equilibrium adsorption isotherms of AY, AB and AG onto MWCNT at 298 K.

The Langmuir model is one of the most often used to describe nonlinear experimental data of adsorption isotherms [11, 12-15] and was fitted to the experimental data. Langmuir theory proposes that adsorption occurs on a homogeneous surface whose adsorption sites are identical and energetically equivalent. Each surface site adsorbs only one molecule, and the energy is equivalent at all sites for the adsorption of one adsorbent molecule, regardless of the presence or absence of other molecules on contiguous sites. This model proposes that a monolayer of adsorbate molecules forms at the interface and no lateral interaction between these molecules occur. The linear form of the Langmuir isotherm equation is represented by:

$$\Gamma = \frac{\Gamma_{max}K_LC_e}{1+K_LC_e} \tag{2}$$

where C_e is the equilibrium concentration of the dye (mg mL^{-1}), Γ is the amount of dye adsorbed (mg g^{-1}), K_L and Γ_{max} are Langmuir constants related to the affinity of the binding sites (adsorption energy) and maximum monolayer adsorption capacity, respectively. The value of Γ_{max} specifies the theoretical saturation capacity of the monolayer and demonstrates that further adsorption will contribute to a prohibitive increase in the Gibbs free energy of the interface. Equation 3 shows the linearized form of the Langmuir model:

$$\frac{C_e}{\Gamma} = \frac{1}{\Gamma_{max}}C_e + \frac{1}{K_L\Gamma_{max}} \tag{3}$$

A plot of C_e/Γ versus C_e enables the calculation of K_L and Γ_{max} from the intercept and slope of the data linear regression, respectively. Table **1** shows the values of Langmuir constants calculated from the intercept and slope of the linear plot for each dye on MWCNT.

Table 1: Coefficients of the Langmuir Model Fitted for AY, AB and AG on MWCNT at 298 K

Adsorbate	Γ_{max} (mg g^{-1})	K_L (g mg^{-1})	R^2
Acid yellow 42	337.84	190.21	0.99345
Acid black 210	328.95	58.72	0.99002
Acid green 68:1	294.12	23.11	0.99768

All isotherms shown in Figure **3** confirm the formation of a monolayer coverage, since all data were very well fitted by the Langmuir isotherm model ($R^2 >$ 0.99). The constants Γ_{max} and K_L indicate the same tendency demonstrated by the isotherms: AY presents higher adsorption than AB, which, in turn, presents higher adsorption than AG. This order suggests that molecular structure of adsorbates may affect adsorption mechanism.

3.3. Thermodynamic Study

Thermodynamic parameters, *i.e.*, the change in Gibbs free energy of adsorption ($\Delta_{ads}G°$), the change in enthalpy of adsorption ($\Delta_{ads}H°$) and the change in entropy of adsorption ($\Delta_{ads}S°$), were estimated to assess the nature of interactions on the adsorption between azo dyes and CNTs. The Gibbs standard free energy change is related to the equilibrium constant ($K°$) by the following equation:

$$\Delta_{ads}G^o = -RTlnK^o \tag{4}$$

where $K°$ is the equilibrium constant of the adsorption process, R is the universal gas constant (8.314 J K^{-1} mol^{-1}), and T is the temperature in Kelvin. The equilibrium constant for the adsorption process, $K°$, is obtained when $\mu_i^{int} = \mu_i^{sol}$, and $\mu_{i\,sol,or,int} = \mu_i^o + RTlna_{i\,sol,or,int}$, in which μ_i^{int} is the chemical potential of i (*i.e.*, the azo dye) adsorbed at the MWCNT–solution interface; μ_i^{sol} is the chemical potential of i in solution (at equilibrium); μ_i^o is the chemical potential of i at a standard condition; and $a_{i\,sol,or,int}$ is the activity of i (in solution or at the MWCNT–solution interface). After some manipulation of the equations, the following relationship is obtained:

$$K^o = \frac{a_i^{int}}{a_i^{sol}} = \frac{\gamma_i^{int}c_i^{int}}{\gamma_i^{sol}c_i^{sol}} \tag{5}$$

where C_i^{int} is the concentration of the adsorbed dye at the MWCNT-solution interface (mg g^{-1}), C_i^{sol}, is the concentration of dye in solution at equilibrium (mg mL^{-1}), γ_i^{int} is the activity coefficient of the adsorbed dye and γ_i^{sol} is the activity coefficient of the dye in solution at equilibrium.

In dilute solutions with low surface coverage, the activity coefficients approach unity, thereby reducing Eq. (5) to:

$$K^o = \frac{c_i^{int}}{c_i^{sol}} = \frac{\Gamma}{C_e} \tag{6}$$

The values of ln $K°$ can be obtained by plotting ln(Γ/C_e) *versus* C_e and by extrapolating C_e to zero. A straight line can be fitted to the points based on a least-squares analysis. Its intercept with the vertical axis yields the values of ln $K°$ that are used in Eq. (4).

It is also known that the Gibbs free energy change is related to the changes in enthalpy and entropy at constant temperature by the following equation:

$$\Delta_{ads}G^o = \Delta_{ads}H^o - T\Delta_{ads}S^o \tag{7}$$

The combination of Eq. (7) and Eq. (4), gives:

$$lnK^o = -\frac{\Delta_{ads}H^o}{RT} + \frac{\Delta_{ads}S^o}{R} \tag{8}$$

$\Delta_{ads}H°$ and $\Delta_{ads}S°$ can then be calculated from the slope and intercept of the van't Hoff plots of ln K° *versus* 1/T, respectively. Table **2** shows these thermodynamic parameters estimated from the adsorption of AY, AB and AG on MWCNT.

Table 2: Thermodynamic Properties Obtained by Van't Hoff Approximation of Adsorption of Azo Dyes on MWCNT

Dyes	$\Delta_{ads}G°/$ kJ mol^{-1}	$\Delta_{ads}H°/$ kJ mol^{-1}	$T\Delta_{ads}S°/$ kJ mol^{-1}
Acid yellow 42	-31.88	49.86	81.74
Acid black 210	-26.04	69.75	95.79
Acid green 68:1	-20.82	55.76	76.58

The adsorption of azo dyes onto MWCNT is a spontaneous process ($\Delta_{ads}G° < 0$) and thermodynamic favorability follows the order of $\Delta_{ads}G°$: AY > AB > AG.

The values of enthalpy change ($\Delta_{ads}H°$) confirm that the adsorptions of all azo dyes on MWCNT are endothermic phenomena, and further support is given by the increase of adsorption capacity with increasing temperature.

The positive value of $\Delta_{ads}S°$ shows that the driving force of the process is the entropy change, described as the increase in the degrees of freedom at the solid-liquid interface during adsorption of azo dyes onto MWCNT. Desolvation of AY, AB and AG molecules and the MWCNT surface during adsorption may cause this phenomenon, due to the increase in the configurational entropy of water molecules at the liquid bulk phase.

Only a few investigations have reported the interaction of dyes and carbon nanotubes. Yan *et al*. show that methylene blue interacts with the SWCNT through charge-transfer and hydrophobic interactions [23]. Liu *et al*. reported that two main factors have been found to play the key roles for the dye-MWCNT interactions: molecular geometry and charge. It was proposed that molecules with planar structures and higher charge load favored the adsorption [24]. In our work, the thermodynamic properties calculated by van't Hoff approximation show that the interactions presented in the adsorption of azo dyes onto MWCNT may not drive to spontaneity, due to the endothermic nature of the process.

3.4. Effect of Ionic Strength

Since large amounts of salts are applied in the dyeing process, the effect of ionic strength on the adsorption was evaluated by examining any changes in the isotherms [13, 21]. Figures **4a**, **4b** and 4c present

the influence of the ionic strength on the adsorption of acid yellow 42, acid black 210 and acid green 68:1, respectively, at three distinct sodium chloride concentrations.
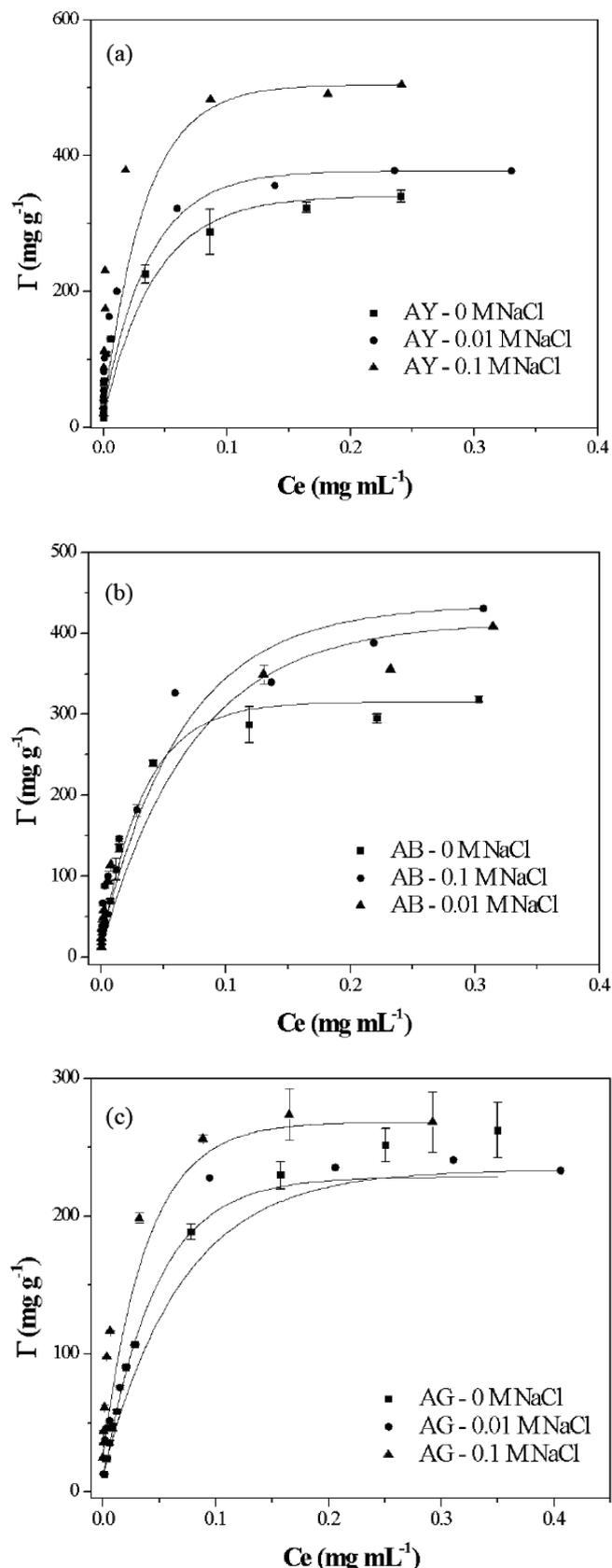

Figure 4: Effect of ionic strength on the adsorption isotherms of AY (**a**), AB (**b**) and AG at 298 K.

The increase in ionic strength causes an increase in the amount of adsorption of azo dyes onto MWCNT. The higher adsorption capacity of CNTs upon salt addition can be attributed to the aggregation of dye molecules induced by the action of salt ions, *i.e.*, salt ions force dye molecules to aggregate, increasing the extent of adsorption of dyes onto CNTs [13]. The adsorption extent of dyes onto the CNT's surface is also dependent of the so-called screening effect – the CNT may be charged on the surface due to the presence of oxygenated groups, being able to reach neutrality by oppositely charged ions from dissolved salt. The latter effect may be validated if the carbon nanotubes present heterogeneous surface.

On the other hand, ionic strength could alter the aggregation state of MWCNT, leading to a better dispersion in the salt solution, when compared with distilled water. This phenomenon could increase the specific surface area, which may contribute to higher amounts of adsorbed dyes per gram of MWCNT.

The isotherms plateau's observed in all plots on Figures **3**-**5** establish different maximum adsorption capacities among the azo dyes studied. These discrepancies may be attributed to the intensity of affinity of the azo dyes structure to CNT chemical nature at saturation levels of adsorption. As can be seen at Figures **1a**, **1b** and **1c**, all dyes present benzoic rings which may favour a better immobilization at CNT surface due to π-π interactions. However, the degrees of freedom of each dye structure probably determines the variation on entropy contribution to the adsorption capacity at equilibrium.

3.5. Surface Modification – Equilibrium and Thermodynamic Studies

Isotherms of adsorption of acid yellow 42 on MWCNT-acid, MWCNT-oxid and pristine MWCNT at 298 K are presented in Figure **5**. The adsorption capacity of the different adsorbents follows the order: MWCNT > MWCNT-oxid > MWCNT-acid, so the surface modification of MWCNT decreased the amount of adsorbed dye in comparison with pristine MWCNT. The order also shows that nitric acid treatment enables a more intense modification of the MWCNT surface than hydrogen peroxide treatment, in comparison with pristine MWCNT.

The decrease in the extent of AY adsorption may be explained by the presence of oxygenated functional groups at the CNTs modified surfaces, which can affect, even minimally, the adsorptive properties of the adsorbent [18]. The surface of pristine CNT is supposed to be more homogeneous, with delocalized π-electrons that enhance the adsorption capability of

aromatic compounds, when compared with other carbon-based adsorbents. Several works indicate that the so-called π-π dispersion forces are responsible for the adsorption of aromatic compounds onto CNT [22]. Oxidation may introduce oxygenated functional groups on the CNT surface, thereby creating a hydrophilic environment [14] and inhibiting adsorption of aromatic compounds by π-π dispersion forces [18]. Another explanation is that the adsorption of water molecules occurs on the oxidized sites of the modified CNT by means of hydrogen bonding [20], which is the so-called "solvent effect". In a previous work, we suggested that specific interactions of phenolic molecules (aromatic compounds) with functional groups that are chemisorbed onto the surface of the MWCNTs (probably hydrogen bonds) are the driving force of the adsorption process [26]. Therefore, the solvent effect and the oxidation of MWCNTs, by the introduction of new functional groups on the adsorbent surface, inhibit the adsorption of azo dyes due to the localization of the π-electron on the adsorbent surface.
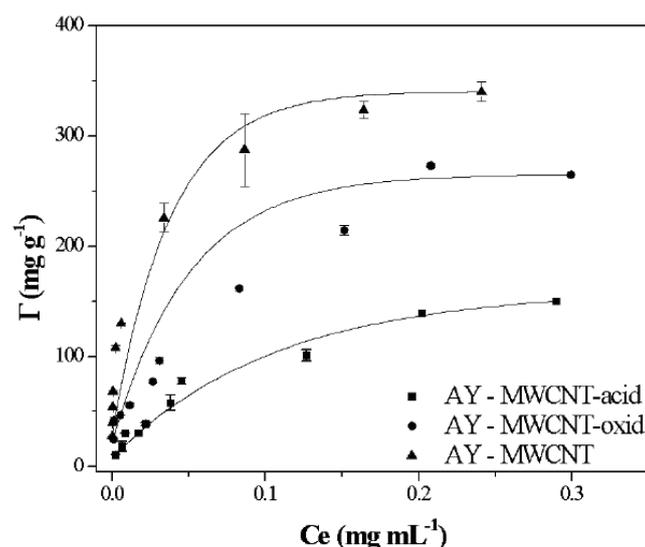

Figure 5: Adsorption isotherms of AY onto MWCNT-acid, MWCNT-oxid and pristine MWCNT at 298 K.

3.5. Microcalorimetry Studies

The energy released or absorbed as heat in a thermodynamic process can be measured by calorimetric techniques that allow their detection. Among these, Isothermal Titration Microcalorimetry (ITC) has been widely used in the characterization of many molecular processes due its high sensitivity, with the possibility of detecting energy flows in the order of 10^{-9} J occurring in a given process.

Curves of variation of the enthalpy of adsorption ($\Delta_{ads}H$) versus the equilibrium concentration of AY, AB and AG on MWCNT obtained from ITC measurements at 298 K are shown in Figure **6**.
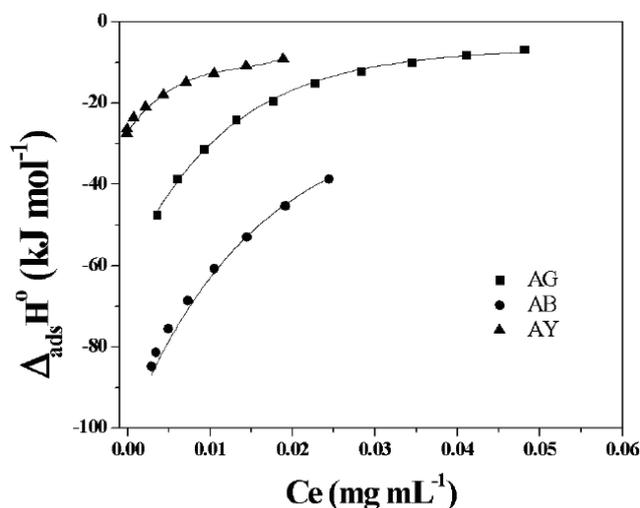
Figure 6: $\Delta_{ads}H$ (kJ mol^{-1}) versus equilibrium concentration (mg mL^{-1}) for the adsorption process of AY, AB and AG on MWCNT.

The van't Hoff model (Equation 8) describes the variation of enthalpy as a function of temperature changes. This theoretical relation assumes that the enthalpy change is constant over a wide range of temperatures even at adsorption equilibrium studies. It means that the interactions established between the azo dyes and CNTs are due to an unique type, where the CNT surface may be chemically uniform.

According to Equation (9), the $\Delta_{ads}H$ values reflect the contributions of five processes: the $\Delta_{deh}H_{AD-H_2O}$ and the $\Delta_{deh}H_{MWCNT-H_2O}$, which are the enthalpy changes of dehydration for the specific azo dye and MWCNT, respectively (both endothermic); the exothermic $\Delta_{int}H_{H_2O-H_2O}$ that is related to the interaction between water molecules released during the desolvation process; $\Delta_{int}H_{AD-AD(MWCNT)}$ (exothermic or endothermic), which describes the interaction energy between molecules of the azo dye adsorbed onto adjacent sites on the MWCNT surface; and the exothermic $\Delta_{int}H_{MWCNT-AD}$, which indicates the intensity of the enthalpic interaction between the dye molecules and the carbon nanotube surface. It is well known that the values of $\Delta_{deh}H_{AD-H_2O}$, $\Delta_{int}H_{AD-AD(MWCNT)}$ and $\Delta_{int}H_{MWCNT-AD}$ differ from one dye compound to another.

$$\Delta_{ads}H = \Delta_{deh}H_{AD-H_2O} + \Delta_{des}H_{MWCN-H_2O} + \Delta_{int}H_{H_2O-H_2O} + \Delta_{int}H_{AD-AD(MWCNT)} + \Delta_{int}H_{MWCNT-AD} \qquad (9)$$

According to Figure **6**, the negative values of $\Delta_{ads}H$ indicate the exothermic nature of all adsorption processes and, upon each injection, $\Delta_{ads}H$ tends to approach zero at higher levels of the equilibrium concentration of dye. At the beginning of the adsorption process, the amount of energy released as heat ($\Delta_{ads}H$) follows the order: AB > AG > AY. As C_e reaches higher values, the change of enthalpy of adsorption becomes

less negative, which confirms the presence of distinct sites on the MWCNT surface that are capable of interacting distinctly with the azo dyes. This evidence shows that the heterogeneity of the MWCNT surface influences the adsorption process, due to electrostatic interactions between the functional groups on the surface and the charged groups of the azo dyes.

Electrostatic interactions and $\pi-\pi$ dispersion forces may occur simultaneously, explaining the general mechanism of adsorption, and the balance between them may be modulated by the chemical structure of the azo dye. In fact, Wang *et al*. recently reported that electronic attraction and $\pi-\pi$ interaction are involved in dye adsorption, and $\pi-\pi$ interaction was the major driving force of the process [25].

Table **3** lists the values of thermodynamic properties obtained by ITC. Contrasting with those estimated by the van't Hoff approximation, the negative values of $\Delta_{ads}H°$ confirm an exothermic process of adsorption. The negative values of $\Delta_{ads}S°$ to AB and AG adsorption indicate a decrease in the entropy change for the adsorbate molecules at the MWCNT-solution interface, caused by a reduction in the configuration entropy of the azo dye molecular structure. Therefore, adsorption of AB and AG onto MWCNT is an enthalpically driven process. On the other hand, the positive value of $\Delta_{ads}S°$ for the adsorption of AY on MWCNT denotes an increase in the entropy change for those molecules at the MWCNT-solution interface, due to the enlargement in the configuration entropy of the dye molecules. In this case, both contributions of enthalpy change and entropy change of adsorption determine the thermodynamic spontaneity of the process.

Table 3:   Thermodynamic properties of the adsorption of azo dyes on MWCNT obtained by ITC

Dyes	$\Delta_{ads}G°/$ kJ mol^{-1}	$\Delta_{ads}H°/$ kJ mol^{-1}	T$\Delta_{ads}S°/$ kJ mol^{-1}
Acid yellow 42	-31.88	-26.87	5.01
Acid black 210	-26.04	-100.06	-74.02
Acid green 68:1	-20.82	-60.70	-39.88

The data in Table **3** also prove that van't Hoff approximation provides an incomplete and erroneous interpretation of the interactions between the azo dyes studied and MWCNTs. The ITC technique seems to present more reliable results, even in terms of the chemical heterogeneity on the CNT's surfaces. Furthermore, it is suitable to provide a good understanding of the surface chemistry of carbon-based adsorbents, such as carbon nanotubes.

4. CONCLUSIONS

This work proposes, for the first time, the use of isothermal titration calorimetry (ITC) to evaluate the surface of a MWCNT sample and the nature of its interactions with azo dyes compounds. The adsorption of acid yellow 42, acid black 210 and acid green 68:1 was evaluated using thermodynamic properties obtained by ITC and van't Hoff approximation. The adsorption of all azo dyes onto MWCNT is spontaneous ($\Delta_{ads}G° < 0$). Adsorptions of AB and AG onto MWCNT are enthalpically driven, while AY is adsorbed by contributions of both enthalpy and entropy changes according to ITC measurements. Calorimetric results show that interactions between azo dyes and MWCNT occur at different sites, and electrostatic interactions and $\pi-\pi$ dispersion forces may occur simultaneously, explaining the general mechanism of adsorption. The balance between them may be modulated by the chemical structure of the azo dye.

It has been demonstrated that the Langmuir model provides good fittings to experimental data ($R^2 > 0.99$), although its theoretical background does not explain the results obtained by ITC. The van't Hoff approximation provides an incomplete and erroneous interpretation of the interactions between the azo dyes studied and MWCNTs.

This work also shows, for the first time, that the ITC technique can be applied to describe the surface of a MWCNT sample, and to elucidate its interactions with adsorbed azo dyes molecules.

ACKNOWLEDGMENTS

FUNDING DECLARATION

CONFLICTS OF INTEREST

The authors declare that there is no conflict of interest regarding the publication of this research article. The funding organizations had no role in the design of the study; in the collection, analysis, or interpretation of data; in the writing of the manuscript; or in the decision to publish the results.

REFERENCES

[1]   Machado FM, Bergmann CP, Fernandes THM, Lima EC, Royer B, Calvete T, Fagan SB. Adsorption of Reactive Red M-2BE dye from water solutions by multi-walled carbon nanotubes and activated carbon. J Hazard Mater 2011; 192(3): 1122-31.
https://doi.org/10.1016/j.jhazmat.2011.06.020

[2]   Nethaji S, Sivasamy A. Adsorptive removal of an acid dye by lignocellulosic waste biomass activated carbon: Equilibrium and kinetic studies. Chemosphere 2011; 82(10): 1367-72.
https://doi.org/10.1016/j.chemosphere.2010.11.080

[3]   Wang L. Application of activated carbon derived from 'waste' bamboo culms for the adsorption of azo disperse dye: Kinetic, equilibrium and thermodynamic studies. J Environ Manage 2012; 102: 79-87.
https://doi.org/10.1016/j.jenvman.2012.02.019

[4]   Jiang R, Fu YQ, Zhu HY, Yao J, Xiao L. Removal of methyl orange from aqueous solutions by magnetic maghemite/chitosan nanocomposite films: Adsorption kinetics and equilibrium. J Appl Polym Sci 2012; 125: E540-49.
https://doi.org/10.1002/app.37003

[5]   Mahmoodi NM, Najafi F. Preparation of surface modified zinc oxide nanoparticle with high capacity dye removal ability. Mater Res Bull 2012; 47: 1800-09.
https://doi.org/10.1016/j.materresbull.2012.03.026

[6]   Zahra A, Imran M, Kanwal F. Comparative Adsorption Studies of Methyl Orange Using Different Varieties of Melon Seeds as Adsorbents. Asian J Chem 2012; 24(6): 2668-70.

[7]   Wang F, Li C, Yu JC. Hexagonal tungsten trioxide nanorods as a rapid adsorbent for methylene blue. Sep Purif Technol 2012; 91: 103-07.
https://doi.org/10.1016/j.seppur.2011.12.001

[8]   Zhao S, Zhou F, Li L, Cao M, Zuo D, Liu H. Removal of anionic dyes from aqueous solutions by adsorption of chitosan-based semi-IPN hydrogel composites. Composites: Part B-Eng 2012; 43(3): 1570-78.
https://doi.org/10.1016/j.compositesb.2012.01.015

[9]   Hameed BH, Ahmad AL, Latiff KNA. Adsorption of basic dye (methylene blue) onto activated carbon prepared from rattan sawdust. Dyes Pigments, 2007; 75: 143-49.
https://doi.org/10.1016/j.dyepig.2006.05.039

[10]   Mane VS, Mall ID, Srivastava VC. Use of bagasse fly ash as an adsorbent for the removal of brilliant green dye from aqueous solution. Dyes Pigments, 2007; 73: 269-78.
https://doi.org/10.1016/j.dyepig.2005.12.006

[11]   Yao Y, Xu F, Chen M, Xu Z, Zhu Z. Adsorption behavior of methylene blue on carbon nanotubes. Bioresource Technol, 2010; 101: 3040-46.
https://doi.org/10.1016/j.biortech.2009.12.042

[12]   Gong JL, Wang B, Zeng GM, Yang CP, Niu CG, Niu QY, ZhouWJ, Liang Y. Removal of cationic dyes from aqueous solution using magnetic multi-wall carbon nanotube nanocomposite as adsorbent. J Hazard Mater, 2009; 164: 1517-22.
https://doi.org/10.1016/j.jhazmat.2008.09.072

[13]   Kuo CY, Wu CH, Wu JY. Adsorption of direct dyes from aqueous solutions by carbon nanotubes: Determination of equilibrium, kinetics and thermodynamics parameters. J Colloid and Interf Sci, 2008; 327: 308-15.
https://doi.org/10.1016/j.jcis.2008.08.038

[14]   Mishra AK, Arockiadoss T, Ramaprabhu S. Study of removal of azo dye by functionalized multi walled carbon nanotubes. Chem Eng J, 2010; 162: 1026-34.
https://doi.org/10.1016/j.cej.2010.07.014

[15]   Wu CH. Adsorption of reactive dye onto carbon nanotubes: Equilibrium, kinetics and thermodynamics. J Hazard Mater, 2007; 144: 93-100.
https://doi.org/10.1016/j.jhazmat.2006.09.083

[16]   Shapour R, Mehrorang G, Kianoosh M. Multiwalled carbon nanotubes as efficient adsorbent for the removal of congo red. Fresen Environ Bull, 2011; 20(10): 2514-20.

[17]   El-Sheikh AH. Effect of oxidation of activated carbon on its enrichment efficiency of metal ions: Comparison with oxidized and non-oxidized multi-walled carbon nanotubes. Talanta, 2008; 75: 127-34.
https://doi.org/10.1016/j.talanta.2007.10.039

[18]   Salam MA, Burk RC. Thermodynamics of pentachlorophenol adsorption from aqueous solutions by oxidized multi-walled carbon nanotubes. Appl Surf Sci, 2008; 255: 1975-81.
https://doi.org/10.1016/j.apsusc.2008.06.168

[19]   Christensen JJ; Hansen LD, Izatt RM. Handbook of proton ionization heats and related thermodynamic quantities; New York: John Wiley and Sons; 1976.

[20]   Dąbrowski A, Podkościelny P, Hubicki Z, Barczak M. Adsorption of phenolic compounds by activated carbon—a critical review. Chemosphere, 2005; 58: 1049-70.
https://doi.org/10.1016/j.chemosphere.2004.09.067

[21]   Liao P, Malik I Z, Zhang W, Yuan S, Tong M, Wang K, Bao, J. Adsorption of dyes from aqueous solutions by microwave modified bamboo charcoal. Chemical Engineering Journal, 195-196, 339-346, 2012.
https://doi.org/10.1016/j.cej.2012.04.092

[22]   Lin D, Xing B. Adsorption of phenolic compounds by carbon nanotubes: role of aromaticity and substitution of hydroxyl groups, Environ. Sci. Technol., 2008; 42: 7254-59.
https://doi.org/10.1021/es801297u

[23]   Yan Y, Zhang M, Gong K, Su L, Guo Z, Mao L. Adsorption of Methylene Blue Dye onto Carbon Nanotubes : A Route to an electrochemically functional nanostructure and its layer-by-layer assembled nanocomposite, Chem. Mater., 2005; 17: 3457-3463.
https://doi.org/10.1021/cm0504182

[24]   Liu CH, Li JJ, Zhang HL, Li BR, Guo Y. Structure dependent interaction between organic dyes and carbon nanotubes, Colloid. Surf. A, 2008; 313: 9-12.
https://doi.org/10.1016/j.colsurfa.2007.04.062

[25]   Wang S, Ng CW, Wang W, Li Q, Hao Z. Synergistic and competitive adsorption of organic dyes on multiwalled carbon nanotubes. Chem. Eng. J., 2012; 197: 34-40.
https://doi.org/10.1016/j.cej.2012.05.008

[26]   R.L. Lavall, C.R. Oliveira, A.B. Mageste, M.C.H. da Silva, L.H.M. da Silva. Adsorção de compostos fenólicos em nanotubos de carbono de paredes múltiplas: uma abordagem termodinâmica. Proceedings of the 34ª Reunião Anual da Sociedade Brasileira de Química; 2012 May 23-26; Florianóplis, Brazil.